A new iterative algorithm for restoration of chromotomographic images*

Andrzej K. Brodzik† and Jonathan M. Mooney‡

† Scientific Software, Woburn, MA 01801
‡ Air Force Research Laboratory, Hanscom AFB, MA 01731

ABSTRACT

We present a new algorithm for chromotomographic image restoration. The main stage of the algorithm employs the iterative method of projections onto convex sets, utilizing a new constraint operator. The constraint takes advantage of hyperspectral data redundancy and information compacting ability of singular value decomposition to reduce noise and artifacts. Results of experiments on both in-house and AVIRIS data demonstrate that the algorithm converges rapidly and delivers high image fidelity.

Keywords: Gerchberg-Papoulis, convex projections, singular value decomposition, image restoration, chromotomography, spectrometry, hyperspectral.

1. INTRODUCTION

Chromotomography provides an estimate of image intensity as a function of position and wavelength. The estimate is based not on a direct measurement of the image, but rather on evaluation of the two-dimensional tomographic projections of the three-dimensional object related to the image via the X-ray transform [21]. The objective of chromotomographic image restoration is to recover the complete three-dimensional spatial-chromatic scene from chromatically sampled two-dimensional projections.

The restoration is obstructed by the *so-called* limited angle problem, generic to many computed-tomography applications, or by the fact that due to certain physical limitations of the measuring instrument not enough data can be collected [1,9,15,20]. Effects of this can be seen in the Fourier domain by appealing to the projection-slice theorem [16]. The theorem states that the two-dimensional Fourier transform of the tomographic projection is equal to the three-dimensional Fourier transform of the image evaluated on a plane through the origin in a direction perpendicular to the projection beam. If a complete set of tomographic projections measured over a full range of angles is not acquired, the union of Fourier transforms of all tomographic projections contains only partial information about the three-dimensional Fourier transform of the object. This is reflected in a singularity of the system transfer function (STF) matrix, which relates the tomographic projections with the object, thus obstructing computation of the hyperspectral image by a direct method of inversion. Use of the pseudoinverse obtained *via* singular value decomposition of the STF matrix offers the minimum norm least square solution; this estimate, however, suffers from poor feature resolution and contains severe artifacts.

In an alternative approach, which bypasses the computation of the pseudoinverse, recovery of the unknown object is achieved by utilizing *a priori* information about the image. Typically, an initial (often arbitrary) guess

*Effort sponsored by the Air Force Office of Scientific Research and Rome Laboratory, Air Force Materiel Command, USAF, under cooperative agreement #F30602-95-2-0034. The U.S. Government is authorized to reproduce and distribute reprints for Governmental purposes notwithstanding any copyright annotation thereon.

about the unknown object is made, which is then subjected to a sequence of corrections, forcing it to satisfy a number of desirable characteristics. This sequence of corrections is applied repetitively until convergence occurs. This technique is known as a method of projections onto convex sets. An example of this approach is the Gerchberg-Papoulis procedure [17], where knowledge of the image spatial boundary and part of its Fourier transform is used to recover the spectral image.

The main challenge of the method of projections onto convex sets is to identify constraint operators that can be easily implemented and that lead to a rapid convergence. This is particularly important, when processing high-dimensionality images, such as hyperspectral data cubes. Traditional constraint operators involving nonnegativity, magnitude bounds, or finite support yield slow convergence and unsatisfactory performance. In this work we propose a new object domain constraint. This constraint is based on the technique of singular value decomposition (SVD), which is used to determine the dominant structure of the data, and to construct reduced-dimensionality approximations by projecting the data onto a subspace that is consistent with image spectral characteristics. Results of experiments demonstrate that the new constraint yields rapid convergence and leads to restoration of a significant portion of the missing information. Since the new algorithm relies on data redundancy, a characteristic of many applications, it is anticipated, that the SVD-POCS algorithm can be effectively applied to other data restoration problems.

The iterative technique proposed in this paper relies on SVD using its various aspects at three different stages of the algorithm: computation of an initial estimate of the unknown image (robust matrix inversion), computation of the object domain constraint (subspace identification), and computation of the transform domain constraint (compaction of information).

The paper is organized as follows: we present an algebraic formulation of the reconstruction problem (Section 2), review the POCS method (Section 3), introduce the new SVD-POCS algorithm (Section 4), and report results of experiments (Section 5).

2. THE PSEUDOINVERSE

An imaging spectrometer reconstructs a three dimensional spatial-chromatic scene from a sequence of two-dimensional images. The reconstruction can be accomplished in several ways, depending on whether multiplexing of information is performed in either the spatial or chromatic domain or jointly. In [13] Mooney has proposed a new computed-tomography image spectrometry technique (chromotomography). In his approach, the multiplexing is accomplished by a rotating prism. As the prism rotates, each chromatic slice of the object cube follows a circular path with the radius of the path determined by the prism dispersion. A sequence of spatial tomographic projections $g(\bar{x},\phi)$ is thus obtained, each tomographic projection being an integral of the three-dimensional spatial-chromatic object cube $f(\bar{x},\lambda)$ in the chromatic variable λ

$$g(\bar{x},\phi) = \int_{-\infty}^{+\infty} f(\bar{x} - k(\lambda-\lambda_0)\bar{p}_\phi, \lambda-\lambda_0)d\lambda, \tag{1}$$

where $\bar{x} = (x_1, x_2)$, $\bar{p}_\phi = (cos\phi, sin\phi)$, $0 \leq \phi < 2\pi$, λ_0 is the center wavelength, and k is a spectrometer constant determined by the sensor focal length and prism dispersion [13]. This can be recognized as a three-dimensional X-ray transform of f with integration performed over a line in direction $k\bar{p}_\phi$, where k determines the angle between the integration line and the optical axis (Fig. 1). Taking the two-dimensional Fourier transform of (1) in the spatial variable $\bar{x}$, we have

$$\mathbf{g}(\bar{\xi},\phi) = \int_{-\infty}^{+\infty} e^{-2\pi i<k\bar{p}_\phi,\bar{\xi}>(\lambda-\lambda_0)}\mathbf{f}(\bar{\xi},\lambda-\lambda_0)d\lambda, \tag{2}$$

where $\mathbf{f}(\bar{\xi},\lambda)$ is the two-dimensional Fourier transform of $f(\bar{x},\lambda)$ in $\bar{x}$, and $\bar{\xi} = (\xi_1,\xi_2)$ is the frequency variable.

Consider a version of (2), sampled at discrete chromatic bands and discrete angles [14]

$$\mathbf{g}_m(\bar{\xi}) = \sum_{n=0}^{N-1} e^{-2\pi i<\bar{p}_m,\bar{\xi}>(n-n_0)}\mathbf{f}_n(\bar{\xi}), \tag{3}$$

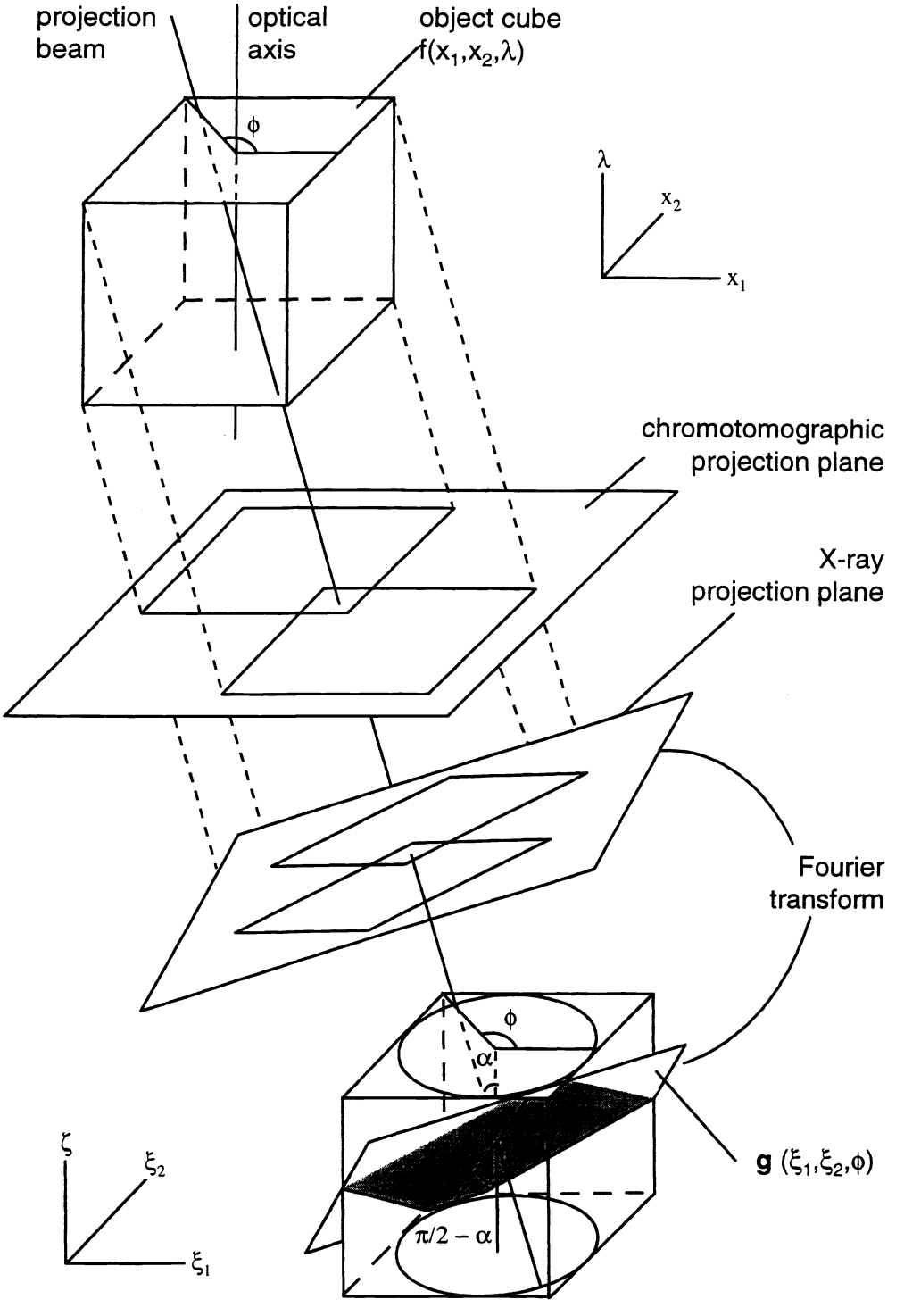

Figure 1: Geometry of chromotomographic data collection and its relation to the X-ray transform.

where $\bar{p}_m = (cos\frac{2\pi m}{M}, sin\frac{2\pi m}{M})$, $0 \leq m < M$, $M \geq N$, $n = k\lambda$, $n_0 = k\lambda_0$, so

$$\begin{bmatrix} g_0(\bar{\xi}) \\ g_1(\bar{\xi}) \\ . \\ . \\ . \\ g_{M-1}(\bar{\xi}) \end{bmatrix} = \mathbf{A}(\bar{\xi}) \begin{bmatrix} f_0(\bar{\xi}) \\ f_1(\bar{\xi}) \\ . \\ . \\ . \\ f_{N-1}(\bar{\xi}) \end{bmatrix} \tag{4}$$

where the $\mathbf{A}(\bar{\xi})$ is an $M \times N$ matrix with elements

$$\mathbf{A}_{m,n}(\bar{\xi}) = e^{-2\pi i <\bar{p}_m, \bar{\xi}> (n-n_0)}. \tag{5}$$

For brevity we write (5) as

$$\mathbf{g} = \mathbf{A}\mathbf{f}. \tag{6}$$

The existence and uniqueness of the solution of (6) depends on the rank of $\mathbf{A}$, which is equal to the number of independent rows of $\mathbf{A}$. It is clear from (5) that $\mathbf{A}$ is ill-conditioned for many values of $\bar{\xi}$. A convenient tool for evaluating the rank of a matrix is singular value decomposition (SVD). The singular value decomposition of a matrix $\mathbf{A}$ is defined as [2]

$$\mathbf{A} = \mathbf{U}\mathbf{\Sigma}\mathbf{V}^{\mathrm{H}}, \tag{7}$$

where $\mathbf{U}$ and $\mathbf{V}$ are $M \times N$ and $N \times N$ matrices, such that

$$\mathbf{U}^{\mathrm{H}}\mathbf{U} = \mathbf{V}\mathbf{V}^{\mathrm{H}} = \mathbf{V}^{\mathrm{H}}\mathbf{V} = \mathbf{I}_N,$$

where superscript H indicates Hermitian adjoint, and $\mathbf{\Sigma}$ is an $N \times N$ diagonal matrix of singular values

$$\mathbf{\Sigma} = diag(\sigma_0, \sigma_1, ..., \sigma_{N-1}),$$

such that $\sigma_0 \geq \sigma_1 \geq ... \geq \sigma_{N-1} \geq 0$. If $\mathbf{A}$ is non-singular, i.e. $\sigma_0 \geq \sigma_1 \geq ... \geq \sigma_{N-1} > 0$, then a matrix inverse to $\mathbf{A}$ can be computed as

$$\mathbf{A}^{-1} = \mathbf{V}\mathbf{\Sigma}^{-1}\mathbf{U}^{\mathrm{H}},$$

where elements of $\mathbf{\Sigma^{-1}}$ are found by inverting elements of $\mathbf{\Sigma}$, and equation (6) has a unique solution given by

$$\mathbf{f} = \mathbf{A}^{-1}\mathbf{g}.$$

If $\mathbf{A}$ is singular, i.e. there is $K < N$ such that $\sigma_0 \geq ... \geq \sigma_{K-1} > \sigma_K = ... = \sigma_{N-1} = 0$, so

$$\mathbf{\Sigma} = \mathbf{\Sigma}_K = diag(\sigma_0, ..., \sigma_{K-1}, 0, ..., 0), \tag{8}$$

then a direct inverse $\mathbf{A}^{-1}$ cannot be obtained and (6) cannot be solved uniquely. Alternatively, the Moore-Penrose inverse (a pseudoinverse) $\mathbf{A}^{+}$ [2] can be used to find a minimum length least square solution of (6). The pseudoinverse of a matrix $\mathbf{A}$ is defined as

$$\mathbf{A}^{+} = \mathbf{V}\mathbf{\Sigma}^{+}\mathbf{U}^{\mathrm{H}}, \tag{9}$$

where the diagonal matrix $\mathbf{\Sigma}^{+}$ is formed by replacing non-zero elements of $\mathbf{\Sigma}$ with the reciprocal values

$$\mathbf{\Sigma}^{+} = diag(\sigma_0^{-1}, ..., \sigma_{K-1}^{-1}, 0, ..., 0). \tag{10}$$

Multiplying both sides of (6) by $\mathbf{A}^{+}$ yields the pseudosolution

$$\mathbf{f}^{+} = \mathbf{A}^{+}\mathbf{g}. \tag{11}$$

In practice the recorded data g is contaminated by noise, i.e.

$$\mathbf{g} = \mathbf{A}\mathbf{f} + \mathbf{n}. \tag{12}$$

In effect, small nonzero singular values of $\mathbf{A}$ result in instabilities. This can be seen by considering

$$\mathbf{A}^{+}\mathbf{g} = \mathbf{A}^{+}\mathbf{A}\mathbf{f} + \mathbf{A}^{+}\mathbf{n} = \mathbf{V}\boldsymbol{\Sigma}^{+}(\boldsymbol{\Sigma}\mathbf{V}^{\mathrm{H}}\mathbf{f} + \mathbf{U}^{\mathrm{H}}\mathbf{n}).$$

If elements of $\boldsymbol{\Sigma}$ are close to zero, then elements of $\boldsymbol{\Sigma}^{+}$ become very large and the filtered noise dominates restoration. In order to balance loss of spectral resolution and noise amplification due to small singular values, a modified version of (10) can be used, where small singular values close to noise variance are set to zero. Alternatively, a regularization technique can be applied, which allows for gradual transition of singular values to zero [19]. Still, the direct method of inversion, as implemented by (11), leads to artifacts in the estimate of the hyperspectral image, particularly in scenes with a significant information content in the low spatial/high chromatic frequency regime. To improve fidelity of the hyperspectral image, one needs to recover the nullspace information. This can be done by using *a priori* information about the scene, such as finite extent, finite intensity range, energy bounds, etc., in the form of solution constraints. If the pseudosolution does not meet these constraints, repetitive application of a sequence of constraints to the estimate leads to recovery of the nullspace information and to reduction of artifacts. The next section describes this technique in detail.

3. PROJECTIONS ONTO CONVEX SETS

The method of projections onto convex sets (POCS) was introduced by Bregman [3] and Gubin *et al* [8] and popularized by Youla and Webb [23], and Sezan, Levi and Stark [11,12,20], who also applied it to image restoration. The method of POCS is an iterative algorithm for finding an image f' in the intersection of a given sequence of R closed convex sets

$$\mathcal{C}_0 = \bigcap_{r=1}^{R} \mathcal{C}_r.$$

A subset $\mathcal{C}$ of $\mathcal{H}$, where $\mathcal{H}$ is a Hilbert space, is *convex*, if for any two of its elements f_1 and f_2 it contains the element $f = \mu f_1 + (1-\mu) f_2$, where $0 \leq \mu \leq 1$. A subset $\mathcal{C}$ of $\mathcal{H}$ is *closed*, if the limit element of any sequence of elements in $\mathcal{C}$ is contained in $\mathcal{C}$. Associated with each closed (not necessarily convex) set $\mathcal{C}_r$ is a projection operator $P_r : \mathcal{H} \rightarrow \mathcal{C}_r$, such that

$$||f - P_r f|| = \min||f - h||, \quad \text{over all } h \in \mathcal{C}_r,$$

so the nearest element to f in $\mathcal{C}_r$ is $P_r f$. If $\mathcal{C}_r$ is convex, then $P_r f$ is unique. Given (in general nonlinear) projection operators P_r associated with closed convex sets $\mathcal{C}_r$ a sequence of images $\{f^k\}$ is generated by the recursive relation

$$f^{k+1} = P_R P_{R-1} \ldots P_1 f^k. \tag{13}$$

The sequence $\{f_k\}$ converges to f' in $\mathcal{C}_0$, i.e. for every $f \in \mathcal{H}$

$$\lim_{k \rightarrow \infty} < f^k, f > = < f', f > .$$

Typical convex sets include sets of images restricted by spatial extent (optical field stop) $\mathcal{C}_{SL}$, known part of the spectrum $\mathcal{C}_{SP}$, band-limitedness $\mathcal{C}_{BL}$, known part of the image $\mathcal{C}_{IP}$, non-negativity, amplitude bound (intensity range), l^2 energy, etc. In the special case when only the two sets $\mathcal{C}_{SL}$ and $\mathcal{C}_{SP}$ are used, the POCS iteration reduces to its famous special case, the Gerchberg-Papoulis algorithm for spectral extrapolation.

The Gerchberg-Papoulis algorithm is one example of the POCS method. Many other algorithms utilizing different constraint sets can be formulated using the framework of POCS, depending on the side information available. This

freedom to match an algorithm to an application is indeed one of the greatest advantages of signal processing approach based on POCS. However, finding useful convex property sets also poses a challenge. The constraints need to describe physical properties of objects with high degree of accuracy. The constraints have to be computationally efficient. Finally, convergence has to be reached in a small number of iterations. The role of the algorithm designer is to identify and implement signal property sets that best fulfill these requirements. Traditional property sets, such as finite spatial extent, amplitude bounds, positivity or spectral limits usually yield slow convergence, partly because the image properties associated with these sets often do not differ significantly from properties of the image estimate. In this paper we introduce two new computationally efficient constraint operators, that lead to a rapidly converging POCS algorithm.

The first constraint set is determined by the data collection system, modeled by means of equations (6) or (11). In either case the SVD of $\mathbf{A}$ leads to partition of the image into two components:

$$\mathbf{f} = \mathbf{f}^+ + \mathbf{f}_N. \tag{14}$$

The pseudoinverse $\mathbf{f}^+$ is the known component of the image to be recovered, corresponding to the non-zero singular values of $\mathbf{A}$. $\mathbf{f}_N$ is the unknown image component, corresponding to the nullspace of $\mathbf{A}$. We will use decomposition (14) to form a constraint set of images with a known part equal to $\mathbf{f}^+$. Since, as will be seen in Section 4, the decomposition takes place in a space spanned by right singular vectors of the system transfer matrix $\mathbf{A}$, we will call this constraint a transform domain constraint.

The second, object domain constraint set is determined directly by the hyperspectral data. It is well known that hyperspectral images are highly redundant, both in the spatial and chromatic variables. The redundant information can be compacted by applying singular value decomposition to the data organized in a matrix form. The compacted information can be extracted from the data matrix and applied as an estimate for the unknown image component $\mathbf{f}_N$.

The following section describes both constraint sets in detail.

4. SVD-POCS ALGORITHM

As it was seen in Section 2, singularity of the system transfer matrix $\mathbf{A}$ leads to parameterization of the solution space by the nullspace of $\mathbf{A}$. Use of the pseudoinverse $\mathbf{A}^+$ yields a unique solution by discarding the nullspace component. Since the pseudoinverse identifies the known data, it can be used to form a constraint set. Indeed, we can write an iteration of the form

$$\mathbf{f}^{k+1} = P_A\mathbf{f} + \bar{P}_A P^f \mathbf{f}^k, \tag{15}$$

where $P_A = \mathbf{A}^+\mathbf{A}$ and $\bar{P}_A = I - \mathbf{A}^+\mathbf{A}$ are the range and nullspace projection operators of $\mathbf{A}$, respectively, and P^f is a projection operator associated with the object domain constraint. In short (15) can be written as

$$\mathbf{f}^{k+1} = \mathbf{f}^+ + \bar{P}_A P^f \mathbf{f}^k \tag{16}$$

$$= P^A P^f \mathbf{f}^k, \tag{17}$$

where $P^A(\mathbf{f}') = \mathbf{f}^+ + \bar{P}_A(\mathbf{f}')$ is a projection of $\mathbf{f}' = P^f\mathbf{f}^k$ onto $\mathcal{C}_A$, a set of signals with a known component $\mathbf{f}^+ = \mathrm{P}_\mathbf{A}\mathbf{f}$. The known part $\mathbf{f}^+$ is used in the iteration as the initial estimate $\mathbf{f}^0$. The unknown component $\mathbf{f}^k$ is iteratively refined by alternately applying projectors P^f and $\bar{P}_A$. Since

$$\mathbf{A}^+\mathbf{A} = \mathbf{V}\mathbf{\Sigma}_\mathrm{K}^+\mathbf{\Sigma}_\mathrm{K}\mathbf{V}^\mathrm{H} = \mathbf{V}I_K\mathbf{V}^\mathrm{H}, \tag{18}$$

where $\mathbf{\Sigma}_\mathrm{K}$ is defined by (8) and I_K is a rank K identity matrix, the iteration (15) can be written as

$$\mathbf{f}^{k+1} = \mathbf{V}I_K\mathbf{V}^\mathrm{H}\mathbf{f} + (I_N - \mathbf{V}I_K\mathbf{V}^\mathrm{H})P^f\mathbf{f}^k. \tag{19}$$

Equation (19) allows us to interpret the constraint projector P^A as a linear filtering operator in a transform space defined by the $\mathbf{V}$ matrix. To see that, premultiply (6) by $\mathbf{\Sigma}^+\mathbf{U}^H$, so that

$$\mathbf{\Sigma}^+\mathbf{U}^H\mathbf{g} = I_K\mathbf{V}^H\mathbf{f}, \tag{20}$$

and set $\mathbf{y} = \mathbf{\Sigma}^+\mathbf{U}^H\mathbf{g}$, and $\mathbf{x} = \mathbf{V}^H\mathbf{f}$. (6) can now be expressed as a simple filtering operation

$$\mathbf{y} = I_K\mathbf{x}. \tag{21}$$

In order to simplify the discussion in this section we have considered a noise-free data collection model (6). The more realistic "data + noise" model of (12) does not affect the derivation or the interpretation of the $\mathbf{V}$-transform constraint in a significant way. Computation of the pseudoinverse, as mentioned in Section 2, has to be modified by setting small singular values to zero to filter out signal components excessively contaminated by noise.

The corner piece of our iterative algorithm for restoration of chromotomographic data is the object domain constraint. The constraint is based on the observation that there exists a significant degree of correlation in hyperspectral images [6,7,10,18]. Since data is redundant, part of the Fourier transform can uniquely represent the hyperspectral image. In chromotomography, the conical shape of the missing data region implies that some information exists for all spatial frequencies and that some information exists for all chromatic frequencies. Using redundancy present in known parts of all horizontal planes (spatial information) and vertical lines (chromatic information) throughout the three-dimensional Fourier cube, we can form an estimate of the unknown image part by forcing the missing data values to be consistent with the known region of the image. Such a data processing approach can be viewed as a subsampling scheme. Since complete Fourier image data acquisition methods are inefficient and sensitive to noise, chromotomographic subsampling combined with SVD-POCS postprocessing of the partially available data provides a viable alternative, where both data collecting efficiency and image fidelity are increased.

The redundancy of a hyperspectral image can be assessed by computing the singular value decomposition of the image organized as a two-dimensional spatial-chromatic matrix. Consider a data matrix

$$F = [f_0, f_1, ..., f_{N-1}]^T, \tag{22}$$

formed by taking as its rows the lexicographically ordered monochromatic slices f_n of the object cube estimate. Application of SVD to F

$$F = U\Sigma V^T = \sum_{n=0}^{N-1} \sigma_n \bar{u}_n \bar{v}_n^T, \tag{23}$$

produces a new set of triples of singular values σ_n, spatial right singular vectors $\bar{v}_n$ (*eigenimages*) and chromatic left singular vectors $\bar{u}_n$ (*eigenchroma*), forming the weighted outer product sum of (23). [1] The eigenimages and eigenchroma are ordered in terms of decreasing singular values, or equivalently, decreasing information.

Typically, a few singular values of the SVD dominate the singular value spectrum (Fig. 2). These singular values correspond to outer products having the richest information content. Since the outer products associated with the lower order singular values represent noise and artifacts, an image can be fully represented by a few top outer products. Specifying *a priori* the number of outer products that represent a hyperspectral image is similar in spirit to constraining a two-dimensional image spatially, as in the Gerchberg-Papoulis procedure. The main factor that differentiates the SVD-POCS algorithm object domain constraint from the Gerchberg-Papoulis algorithm finite spatial extent constraint is that, in the former, information is constrained in an indirect way by selection of the image "feature subspace" spanned by the dominant singular vectors of the data matrix, while in the later the constraint is realized by selection of the image valid spatial indexes. An approach based on the former constraint is both efficient and intuitively pleasing, since selection of the outer products has an immediate and profound effect on the data and affects the entire information content of the spatial-chromatic image, rather than a single aspect of it, spatial boundaries, whose importance is often uncertain.

[1] To distinguish the SVD of the data matrix F from the SVD of the system transfer function matrix $\mathbf{A}$, we use italic letters U, Σ, V for the former, and bold letters $\mathbf{U}, \mathbf{\Sigma}, \mathbf{V}$ for the later.

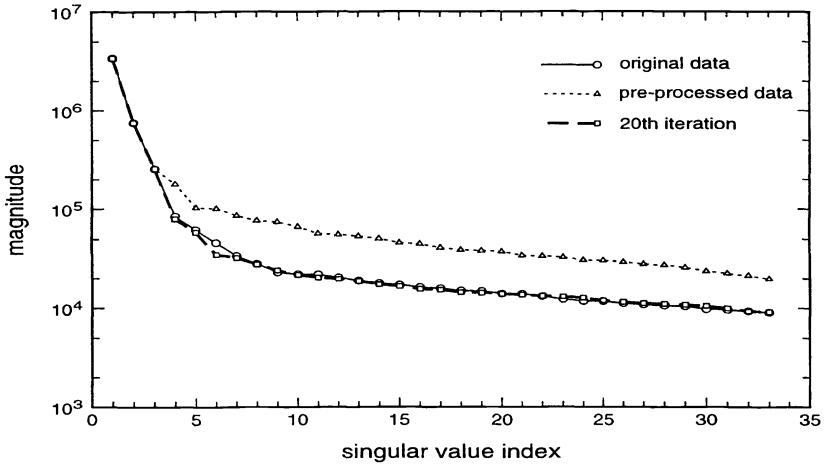

Figure 2: Singular value spectrum of 'Jasper Ridge'.

Define projector $P^f = UI_LU^T$, where U is the eigenchroma matrix of the pseudoinverse $F = F^0$, as in (23), I_L is a rank L identity matrix, and L is the constrained number of eigenimage-eigenchroma pairs of F. The image in (23) can then be decomposed as

$$F = F_L + F_L', \tag{24}$$

where

$$F_L = P^f F. \tag{25}$$

F_L is a projection of F onto the "feature space" U_L, represents the compacted image information and is used as an estimate for the missing part of the spatial-chromatic data. $F_L' = F - F_L$ is the orthogonal complement of F_L, which is a projection of F onto the "noise space" $U - U_L$ and represents noise and artifacts and is discarded.

Selection of the "feature space" dimension L is of great importance, since it bears on fidelity of the restoration and convergence speed of the algorithm. One intuitive approach is to identify an abrupt change in the singular value spectrum, and use it as a demarcation point for subspace decomposition. Initial investigations have shown that this strategy can be fruitful. Optimal selection of the "feature space" dimension, convergence conditions and computational complexity of the algorithm will be addressed elsewhere [4].

5. EXPERIMENTS

We have tested the algorithm on several synthesized and real datasets. Real datasets were either chromotomographic sequences of scenes acquired with a hyperspectral camera built in our lab, and passed through both stages of the algorithm (inverse + iterations), or sample AVIRIS data, preprocessed to mimic the loss of information occurring in the inversion stage, and subjected only to the iteration stage of the algorithm.

To evaluate the performance of the algorithm on complex data, we used a sample AVIRIS image "Jasper Ridge". We selected a 240×240 segment from the original 512×614 image and chose 64 consecutive frames (starting with the 44th frame) from the sequence of 224 to fit our processing environment. We preprocessed the initial set of images, subtracting the low spatial frequency information by multiplying the set by $\mathbf{A}^H\mathbf{A}$. We then applied the iterative algorithm, using the first five eigenimages (representing most of the image energy) to form a reduced-rank data matrix estimate.

Fig. 3 illustrates the progression of the first five eigenimages of the hyperspectral data through the different stages of the algorithm: the original set (first column), the preprocessed set (second column) and the 20-th iterate

(third column). The artifacts evident in the fourth and fifth eigenimage of the preprocessed data (and to a lesser degree in the third eigenimage) largely disappear in the corresponding eigenimages of the 20-th iterate. Similarly, the singular value spectrum of the iterate approaches that of the original image (Fig. 2). The rms error of the 20-th iterate of the first, second and third eigenimage yields a two-, four- and five-fold decrease, respectively, as compared with the rms error of the pre-processed data. Even higher rms error reduction rates occur for the lower order eigenimages.

The second test sequence was obtained with an infrared camera built in our laboratory [15]. The f/4 InSb camera utilizes a 256×256 FPA, and operates in the 3-5 μm band at 60 frames per second with a 2 ms integration time. The camera collects one frame of data for each of the 80 prism orientations, uniformly spaced over 2π. We imaged a target of opportunity (a building) from the laboratory window. The data was obtained on January 12, 1998, at 9.30 a.m. In order to minimize the effects of FPA nonuniformities and stray reflections from the rotating prism, an additional sequence of data was recorded with the entrance pupil blocked. The blocked sequence was used to perform a one-point nonuniformity correction on a 'frame by frame' basis.

Fig. 4 illustrates the top six eigenimages of the scene. The upper half of the figure shows eigenimages of the pseudo-inverted data. All six eigenimages contain reconstruction artifacts in the form of high contrast halos around the building. These halos are characteristic of the high-pass filtering and noise amplification introduced by the pseudoinverse. The lower half of Fig. 4 illustrates the effect of the iterative algorithm on the artifacts; the halos have been eliminated. Incidentally, the eigendecomposition demonstrates the importance of focal plane array nonuniformities, which appear in the third eigenimage.

6. SUMMARY

The objective of this work was the design of an algorithm for improving the quality of the chromotomographic image restoration. The objective was accomplished by introducing a novel object domain constraint based on the inherent redundancy of the hyperspectral data and on the information compacting ability of singular value decomposition. As a result, a highly efficient and effective image restoration algorithm for processing chromotomographic images was obtained. It was demonstrated that the iterative algorithm is able to suppress artifacts and noise characteristic of the pseudosolution, and to improve resolution of the distinct features present in the scene. The algorithm allows one to monitor the progress of iteration in both: a quantitative (singular values) and a qualitative (eigenimages) manner. The computational cost of the iteration was highly reduced by transferring the two-dimensional DFT calculations to the precomputational stage [4]. All three aspects - performance, tractability and efficiency - indicate that the new constraints are far superior to the standard constraints in processing of chromotomographic data.

The main issues to be investigated in the future are the design of an easily computable criterion for determining the degree of hyperspectral model reduction, and validation of the assumption that high order eigenchroma are shared by different spatial frequency regions of the hyperspectral image. The reliability of the model reduction criterion and eigenchroma error estimates are going to impact the performance of the algorithm. Since both the scene chromatic content and the relative importance of various spectral components can be highly dependent upon the application, characterization of a wide range of hyperspectral scenes needs to be performed.

ACKNOWLEDGMENTS

The authors wish to thank Jerry Silverman, Virgil Vickers and Bill Ewing for critical reading of the manuscript, Myoung An and Virgil Vickers for software support, and Linda Bouthillette for the artwork.

BIBLIOGRAPHY

[1] H. H. Barrett, *Limited-angle tomography for the nineties*, J. Nucl. Med., Vol. 31, No. 10, 1689-1692, 1990.

[2] A. Ben-Israel and T. N. E. Greville, *Generalized Inverses: Theory and Applications*, 1980.

[3] L. M. Bregman, *The method of successive projections for finding a common point of convex sets*, Dokl. Akad. Nauk SSSR, Vol. 162, No. 3, 487-490, 1965.

[4] A. K. Brodzik and J. M. Mooney, *SVD-POCS Algorithm for Restoration of Limited Angle Chromotomographic Images*, submitted for publication.

[5] A. K. Brodzik, J. M. Mooney and M. An, *Image Restoration by Convex Projections: Application to Image Spectrometry*, SPIE, Vol. 2819, 231-242, 1996.

[6] N. H. Endsley, *Spectral unmixing algorithms based on statistical models*, SPIE, Vol. 2480, 23-36, 1995.

[7] A. A. Green, M. Berman, P. Switzer and M. D. Craig, *A Transformation for Ordering Multispectral Data in Terms of Image Quality with Implications for Noise Removal*, IEEE Trans. on GRS, Vol. 32, No. 4, 65-74, 1988.

[8] L. G. Gubin, B. T. Polyak, and E. V. Raik, *The method of projections for finding a common point of convex sets*, USSR Computational Mathematics and Mathematical Physics, Vol. 7, No. 6, 1-24, 1967.

[9] D. A. Hayner and W. K. Jenkins, *The missing cone problem in computer tomography*, Advances in computer vision and image processing, Ed. T. S. Huangi, Vol. 1, JAI Press, 83-144, 1984.

[10] J. B. Lee, A. S. Woodyatt and M. Berman, *Enhancement of High Spectral Resolution Remote-Sensing Data by a Noise-Adjusted Principal Component Transform* , IEEE Trans. on GRS, Vol. 28, No. 3, 295-304, 1990.

[11] A. Levi and H. Stark, *Signal restoration from phase by projections onto convex sets*, J. Opt. Soc. Am., Vol. 73, No. 6, 810-822, 1983.

[12] A. Levi and H. Stark, *Image restoration by the method of generalized projections with application to restoration from magnitude*, J. Opt. Soc. Am., Vol. 1, No. 9, 932-943, 1984.

[13] J. M. Mooney, *Spectral imaging via computed tomography*, Proc. IRIS Passive Sensors, 203-215, 1994.

[14] J. M. Mooney, A. K. Brodzik and M. An, *Principal Component Analysis in Limited Angle Chromotomography*, SPIE, 1997.

[15] J. M. Mooney, V. E. Vickers, M. An and A. K. Brodzik, *A High Throughput Hyperspectral Infrared Camera*, J. Opt. Soc. Am. A, Vol. 14, No. 11, 2951-2961, 1997.

[16] F. Natterer, *The Mathematics of Computerized Tomography*, John Wiley Sons, 1986.

[17] A. Papoulis, *A new algorithm in spectral analysis and band-limited extrapolation*, IEEE Trans. on Circuits and Systems, Vol. CAS-22, 735-742, 1975.

[18] P. J. Ready and P. A. Wintz, *Information Extraction, SNR Improvement, and Data Compression in Multispectral Imagery*, IEEE Trans. on Comm., Vol. COM-21, No. 10, 1123-1130, 1973.

[19] A. Sano, *Optimally regularized inverse of singular value decomposition and application to signal extrapolation*, Signal Processing, Vol. 30, 163-176, 1993.

[20] M. I. Sezan and H. Stark, *Image restoration by the method of convex projections: part 2 - applications and numerical results*, IEEE Trans. on Medical Imaging, Vol. MI-1, No. 2, 95-101, 1982.

[21] D. C. Solmon, *The X-ray Transform*, J. Math. Anal. Appl., 56, 61-83, 1976.

[22] K. C. Tam and V. Perez-Mendez, *Tomographic imaging with limited-angle input*, J. Opt. Soc. Am., Vol. 71, No. 5, 582-592, 1981.

[23] D. C. Youla and H. Webb, *Image restoration by the method of convex projections: part 1 - theory*, IEEE Trans. on Medical Imaging, Vol. MI-1, No. 2, 81-94, 1982.

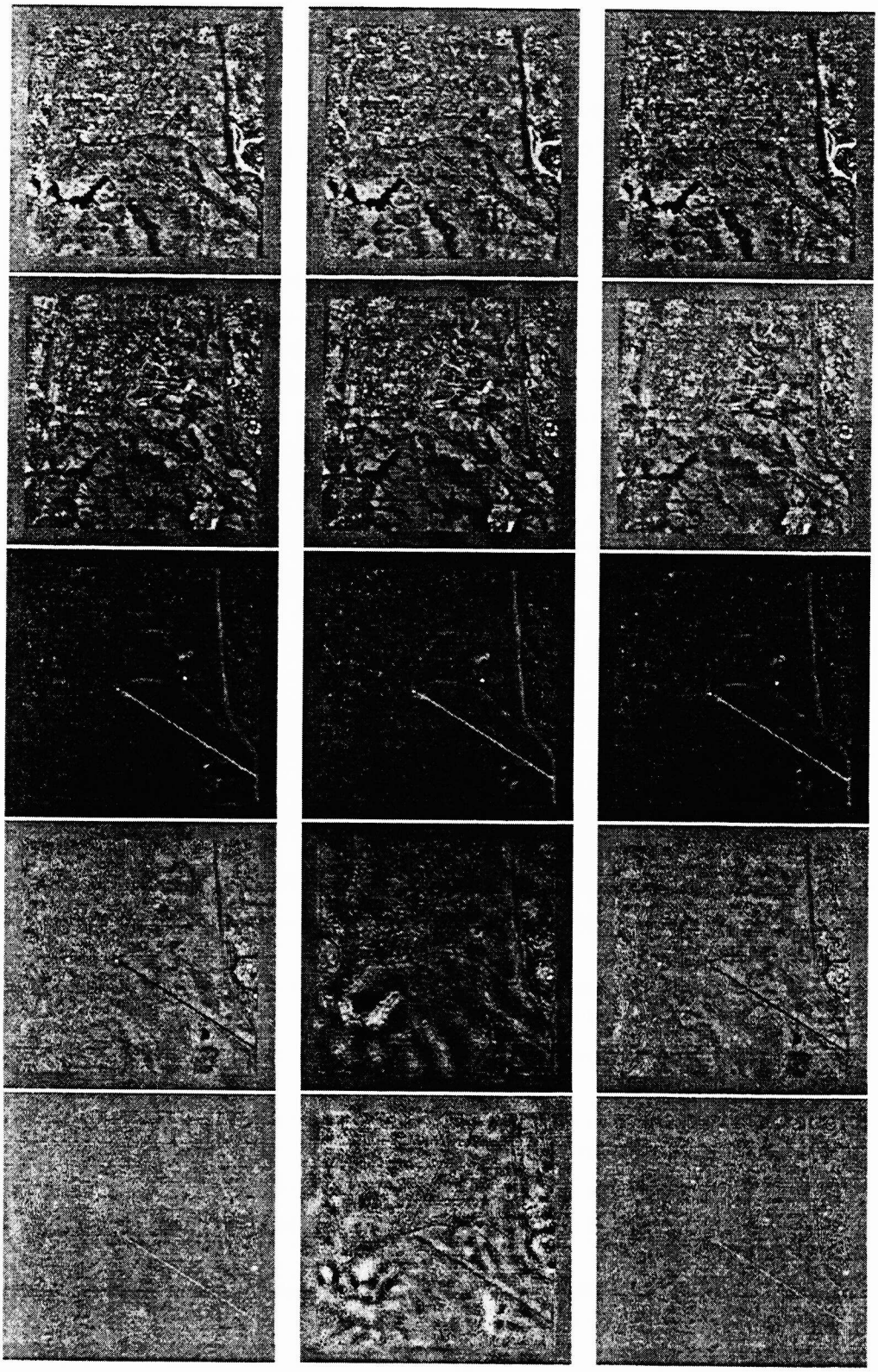

Figure 3: The first five eigenimages of 'Jasper Ridge': the original AVIRIS sequence (first column), the pseudo-inverse reconstruction (second column), and the twentieth iteration (third column).

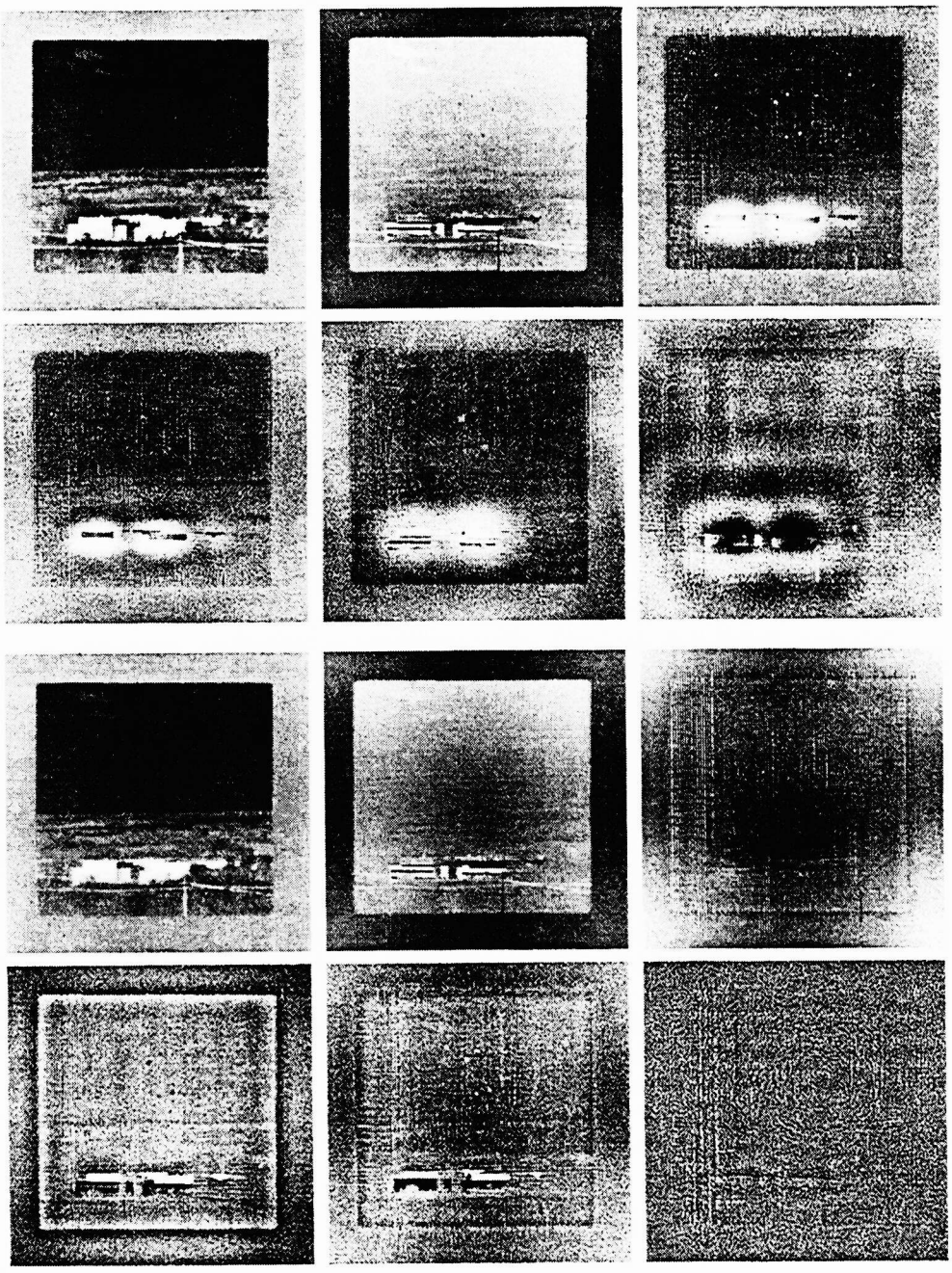

Figure 4: The first six eigenimages of 'Hanscom': the pseudoinverse (the upper half), and the twentieth iteration (the lower half).